

# The Anisotropy of the Reciprocal Form Factor and the Electronic Structure of Crystalline Lithium Hydride\*

Tanja Asthalter and Wolf Weyrich

Fakultät für Chemie, Universität Konstanz, Konstanz, Fed. Rep. of Germany

Z. Naturforsch. **48a**, 303–309 (1993); received January 13, 1993

New high-precision measurements of the isotropic as well as of three directional Compton spectra of lithium hydride have been carried out using  $^{241}\text{Am}$  as a  $\gamma$ -ray source. In order to account for the extreme sensitivity of LiH powder to atmospheric moisture, the final data (i.e. the reciprocal form factor) were corrected for the LiOH content determined by titrimetric analysis. For the interpretation of the data, theoretical calculations were carried out using a Hartree–Fock program for periodic systems (CRYSTAL). Basis sets published by Dovesi et al. were used, one of which allows for polarisation of both the hydride and lithium ions. Comparison of the theoretical data with the experiment shows much better agreement of the results of complete solid-state calculations that take into account higher-order effects (polarisation and covalency) than those obtained by Löwdin orthogonalisation of free-ion wave functions (which assumes pure ionicity, neglecting all but first-order effects). The influence of further polarisation functions on the reciprocal form factor is investigated and discussed. The remaining discrepancies are attributed to electron–electron correlation.

**Key words:** Compton spectroscopy; Reciprocal form factor; Ionic crystal; Electronic structure; Lithium hydride.

## 1. Introduction

The Fourier transform of (directional or isotropic) Compton profiles – the so-called reciprocal form factor  $B(s)$  – directly mirrors the autocorrelation properties of the one-electron wave functions in position space, thus yielding valuable information about the nature of chemical bonding, e.g. in a solid [1–3]. Comparison between highly accurate experimental data and various calculated  $B(s)$  is therefore a powerful tool for testing the validity of different quantum-chemical models for chemical bonding; it has also turned out to yield a sensitive indicator for the quality of basis sets. In particular it is possible to investigate the importance of higher-order vs. first-order bonding effects. Since the Fourier transform of a directional Compton profile is a data vector consisting of the functional values of the three-dimensional  $B(s)$  along a line parallel to the experimental scattering vector, one can discuss bonding effects in different directions separately.

\* Presented at the Sagamore X Conference on Charge, Spin, and Momentum Densities, Konstanz, Fed. Rep. of Germany, September 1–7, 1991.

Reprint requests to Prof. Dr. Dr. h.c. Wolf Weyrich, Lehrstuhl für Physikalische Chemie I, Fakultät für Chemie, Universität Konstanz, Postfach 55 60, D-W-7750 Konstanz, Fed. Rep. of Germany.

LiH as the simplest binary compound that is experimentally accessible in bulk has been the subject of numerous position and momentum density measurements as well as of calculations of the isolated molecule, clusters and the bulk compound (cf. [3–8]). As for the Compton profiles, no quantitative agreement between experiment and various theoretical models has yet been achieved [3, 7, 8].

The aim of our investigations was therefore to eliminate as many experimental errors as possible – to correct for impurities produced by hydrolysis of the LiH powder, to have good counting statistics, and, of course, to account properly for the various systematic errors of the scattering experiment. Only then reliable statements about the validity of various theoretical models become possible.

## 2. Experiment

For the powder measurements, high-purity LiH (99.5%, ESPI, grain size 8–35 mesh) was pulverised in a mortar. The single crystals were provided by the Crystal Growth Laboratory, University of Utah.

The samples were prepared in a glove box with dry air (relative humidity  $\leq 1\%$ ). When cutting the crystals into slices, they were continuously handled under thoroughly dried paraffin.

0932-0784 / 93 / 0100-0303 \$ 01.30/0. – Please order a reprint rather than making your own copy.



Dieses Werk wurde im Jahr 2013 vom Verlag Zeitschrift für Naturforschung in Zusammenarbeit mit der Max-Planck-Gesellschaft zur Förderung der Wissenschaften e.V. digitalisiert und unter folgender Lizenz veröffentlicht: Creative Commons Namensnennung-Keine Bearbeitung 3.0 Deutschland Lizenz.

Zum 01.01.2015 ist eine Anpassung der Lizenzbedingungen (Entfall der Creative Commons Lizenzbedingung „Keine Bearbeitung“) beabsichtigt, um eine Nachnutzung auch im Rahmen zukünftiger wissenschaftlicher Nutzungsformen zu ermöglichen.

This work has been digitalized and published in 2013 by Verlag Zeitschrift für Naturforschung in cooperation with the Max Planck Society for the Advancement of Science under a Creative Commons Attribution-NoDerivs 3.0 Germany License.

On 01.01.2015 it is planned to change the License Conditions (the removal of the Creative Commons License condition “no derivative works”). This is to allow reuse in the area of future scientific usage.

The titrimetric analysis of the LiH powder was carried out using the method described by Kotova et al. [9] before and after each measurement. The powder samples contained a mole fraction of 1.06–1.36% LiOH (weighted mean value), but no carbonate. A  $B(s)$  curve of LiOH (taken from [10]) was then used to correct the LiH raw data.

The spectra were measured under vacuum using a  $^{241}\text{Am}$   $\gamma$ -ray source. Atmospheric moisture was kept off by phosphorus pentoxide. The scattered photons were detected under a scattering angle of  $\varphi = 163.7^\circ$  for the powder and  $159^\circ$  for the single-crystal measurements, using a planar intrinsic Ge detector with pulsed optical feedback (Princeton Gamma Tech). The full width at half maximum of the angular distribution of scattering angles was  $\Delta\varphi_{\text{FWHM}} = 5.6^\circ$  in the powder and  $\Delta\varphi_{\text{FWHM}} = 3.0^\circ$  in the single-crystal measurements. The FWHM of the angular distribution of scattering vectors was  $\Delta\varphi_{k,\parallel} = 3.4^\circ$  within and  $\Delta\varphi_{k,\perp} = 3.9^\circ$  perpendicular to the scattering plane. The overall experimental resolution (detector plus angular distribution of scattering angles) was  $\Delta q_{\text{FWHM}} = 0.58 p_0$  (powder) and  $0.542 p_0$  (single crystals), resp. ( $p_0 = \hbar/a_0 = 1.99289 \cdot 10^{-24} \text{ kg m/s}$ ).

The data processing was performed using a program package based upon correction methods of Weyrich [11] and Bachmann [12]. The reciprocal form factor was obtained by Fourier transformation of the Compton profile in the momentum range  $-11.083 p_0 \leq q \leq +11.083 p_0$ , yielding a stepwidth of  $\Delta s = 0.15 \text{ \AA}$  in the  $s$ -domain. The multiple scattering was corrected for by extrapolating the final results to zero sample thickness [11] with the exception of the range  $s \geq 2.1 \text{ \AA}$  of the single-crystal curves, where the raw data were used because of negligible influence of multiple scattering.

### 3. Theory

Calculations were performed using the Hartree-Fock program for periodic systems "CRYSTAL" of Pisani, Dovesi and Roetti (1988 version, see [13]). The influence of various basis sets on  $B(s)$  in the three directions of close interionic contact,  $\langle 100 \rangle$ ,  $\langle 110 \rangle$ , and  $\langle 111 \rangle$ , was tested. The  $B(s)$  curves were obtained from the density matrix in position representation by making use of the cyclicity of the matrix (translational invariance) and expressing it in terms of basis functions,

$$B(s) = \sum_k \sum_l \sum_g P_{kl}^g \int_{-\infty}^{+\infty} \int_{-\infty}^{+\infty} \int_{-\infty}^{+\infty} \varphi_k(\mathbf{r} - \mathbf{R}_k) \varphi_l^*(\mathbf{r} - \mathbf{R}_l - \mathbf{g} + s) d\mathbf{r}, \quad (1)$$

where  $P_{kl}^g$  are the first-order density matrix elements with respect to the (usually atomic) basis functions  $\varphi_k(\mathbf{r} - \mathbf{R}_k)$  centred at the position  $\mathbf{R}_k$  and  $\varphi_l(\mathbf{r} - \mathbf{R}_l - \mathbf{g})$  located in a unit cell offset by the position-lattice vector  $\mathbf{g}$  and centred there at the position  $\mathbf{R}_l$  relative to the origin of that cell.

For the evaluation of first-order bonding effects [14], a program was written that performs symmetrical Löwdin orthogonalisation [15, 16] of atomic, ionic or molecular wave functions (also generated by CRYSTAL) according to

$$\mathbf{C}' = \mathbf{C} \cdot \mathbf{T}, \quad (2)$$

where

$$\mathbf{T} = \Delta^{-1/2} = (\mathbf{1} + \mathbf{S})^{-1/2} \\ = \mathbf{1} - \frac{1}{2}\mathbf{S} + \frac{3}{8}\mathbf{S}^2 - \frac{5}{16}\mathbf{S}^3 + \frac{35}{128}\mathbf{S}^4 - \dots \quad (3)$$

Here, the non-orthogonal eigenvectors of the fragments to be orthogonalised in the geometrical arrangement of the crystal are written as  $\mathbf{C} = \{\mathbf{c}_\mu\}$ , the orthogonalised ones by  $\mathbf{C}' = \{\mathbf{c}'_\mu\}$ ;  $\mathbf{T}$  is the unitary transformation matrix, and  $\Delta$  is the metric matrix containing the overlaps of totally  $N$  (spin) orbitals  $\psi_\mu$  with eigenvectors  $\mathbf{c}_\mu$  in the representation of totally  $m$  basis functions:

$$\mathbf{C} = \{\mathbf{c}_1, \mathbf{c}_2, \dots, \mathbf{c}_N\}, \quad \mathbf{c}_\mu = \begin{pmatrix} c_{1\mu} \\ c_{2\mu} \\ \vdots \\ c_{m\mu} \end{pmatrix}, \quad (4)$$

$$\Delta = \{\Delta_{\mu\nu}\}_{N,N}, \quad \Delta_{\mu\nu} = \int_{-\infty}^{+\infty} \int_{-\infty}^{+\infty} \int_{-\infty}^{+\infty} \psi_\mu^*(\mathbf{r}) \psi_\nu(\mathbf{r}) d\mathbf{r}. \quad (5)$$

Convergence of the series expansion (3) was ensured by the scaling method given by Löwdin in 1956 [16].

### 4. Results and Discussion

Although the mole fraction of LiOH in the samples never exceeded 1.4%, the correction to the reciprocal form factor  $B(s)$  turned out to be non-negligible in the range of  $0 \leq s \leq 1 \text{ \AA}$  owing to the greater number of electrons per formula unit of LiOH in comparison to LiH and the faster decaying oxygen core contribution to  $B(s)$  (Figure 1). Only when this correction is included, the powder  $B(s)$  curve is very close to the mean value of the directional  $B(s)$  over the whole range of  $s$ . In the range of larger  $s$ -values, however,  $B(s)$  is not affected significantly.

The comparison between the various crystallographic directions shows that the anisotropy of the

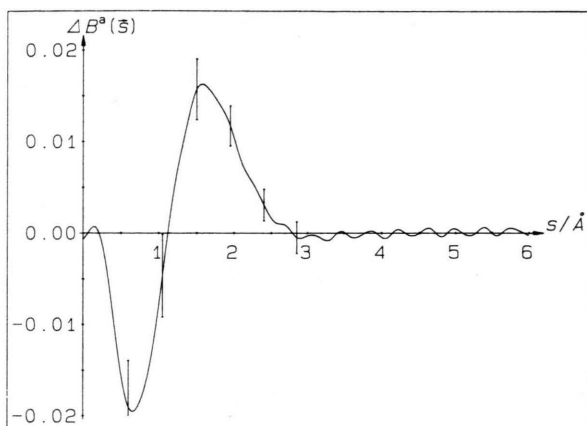


Fig. 1. Influence of the correction for LiOH impurities on the spherically averaged reciprocal form factor of LiH; the difference curve  $\Delta B^s(s) \equiv B^s(s)_{\text{corr}} - B^s(s)_{\text{uncorr}}$  is shown.

Table 1. Exponents and contraction coefficients for the hydride-ion basis set.

Function type	Exponent/ $a_0^{-2}$	Coefficient
s	128.000	$2.8 \cdot 10^{-6}$
	64.000	$7.3 \cdot 10^{-5}$
	32.000	$1.6 \cdot 10^{-3}$
	16.000	$4.3 \cdot 10^{-4}$
	8.000	$8.1 \cdot 10^{-3}$
	4.000	$4.6 \cdot 10^{-3}$
	2.000	$2.8 \cdot 10^{-2}$
	0.800	$7.0 \cdot 10^{-2}$
s	0.400	0.055
	0.280	0.32
	0.070	0.73
s	0.035	1.0
s	0.010	1.0

reciprocal form factor is smaller than was suggested by earlier theoretical investigations (Berggren [4] and Aikala [6], analysed in [3]), which were limited to the orthogonalisation of the wave functions of isolated ions in the geometrical arrangement of the crystal structure (first-order interactions, see above). Nevertheless, still the most negative orbital autocorrelation occurs in the  $\langle 110 \rangle$ -direction, where the overlap between the diffuse charge distributions of adjacent hydride ions reaches a maximum with respect to the other directions (for a detailed discussion, see [3]).

The assessment of higher-order effects by direct comparison between Aikala's data and the present CRYSTAL results, however, is complicated by two

further effects that are due to the employed basis sets and that must be minimised or taken into account:

1. The different shape of Slater- and Gaussian-type orbitals might produce different artefacts in  $B(s)$ . Therefore, as indicated above, Gaussian wave functions for the free ions were used to perform Löwdin orthogonalisation. For the  $\text{Li}^+$  ion, a basis set of Sasagane et al. [17] was used. The resulting total energy differs only by  $10^{-3} E_h$  from the value of  $-7.2364121 E_h$  given by Clementi [18]. For the  $\text{H}^-$  ion, a basis set was developed that yields a total energy of  $-0.4870899 E_h$  (Hartree-Fock limit:  $-0.4879297 E_h$  [19]). Its exponents and coefficients are listed in Table 1.

2. In order to eliminate the basis-set superposition error (BSSE, [20, 21]), the free-ion wave functions ought to be corrected, e.g. by the counterpoise method. A check of the BSSE in the reciprocal form factor of the free ions with the basis sets mentioned above was therefore performed and found to be insignificant over the whole  $s$ -range, compared to the experimental error.

All  $B(s)$  curves in this paper – experimental and theoretical ones – are attenuated with a Gaussian function  $G(s) = \exp[-(s/3.2514 \text{ Å})^2]$ ,

$$B^a(s) = B(s) \cdot G(s), \quad (6)$$

which corresponds to a standardised experimental resolution in the momentum domain of  $\Delta q_{\text{FWHM}} = 0.542 p_0$ . The numerical values of the  $B^a(s)$  and  $B^b(s)$  and the statistical precision of the experimental data are given in Tables 2–5. By inversion of (6), unattenuated values are easily obtained. The experimental error margins, however, increase with  $1/G(s)$  in that case.

Figures 2–4 show the experimental directional curves together with Aikala's data for SOSTIOs (symmetrically orthogonalised Slater-type ion orbitals) and the new data for SOGTIOs (symmetrical orthogonalised Gauss-type ion orbitals) as well as with the CRYSTAL results using the best-possible basis set (EBS, see [8]).

In order to demonstrate how the crystal basis set influences the quality of  $B(s)$ , the results of CRYSTAL calculations of the three directional reciprocal form factors ( $\langle 100 \rangle$ ,  $\langle 110 \rangle$ , and  $\langle 111 \rangle$ ) are shown in Figs. 6–8, again with the experimental data as a reference.

The quality of the free-ion and crystal basis sets varies as follows:

- The free-ion basis sets for our SOGTIOs are the one of Sasagane et al. [17] for  $\text{Li}^+$  and the one given in Table 1 for  $\text{H}^-$ , as already mentioned;

Table 2.  $B^a(s)$  of LiH, spherical average, experiment vs. theory. Experimental error:  $8.9 \cdot 10^{-4} (s > 2 \text{ \AA}) \leq \sigma \leq 4.9 \cdot 10^{-3} (s = 0.75 \text{ \AA})$ .

$s/\text{\AA}$	$B^a(s)$				
	uncorr.	corr.	MCS	EBS	EBS+d
0.00	3.9978	3.9972	4.0000	4.0000	4.0000
0.15	3.6963	3.6970	3.7946	3.7973	3.7973
0.30	3.1828	3.1798	3.3217	3.3375	3.3376
0.45	2.6682	2.6559	2.7847	2.8175	2.8176
0.60	2.2120	2.1930	2.2931	2.3379	2.3380
0.75	1.8273	1.8088	1.8806	1.9284	1.9284
0.90	1.5005	1.4869	1.5426	1.5875	1.5875
1.05	1.2245	1.2199	1.2639	1.3035	1.3034
1.20	0.9890	0.9937	1.0312	1.0637	1.0635
1.35	0.7899	0.8009	0.8347	0.8589	0.8586
1.50	0.6183	0.6340	0.6657	0.6832	0.6828
1.65	0.4766	0.4925	0.5233	0.5329	0.5325
1.80	0.3581	0.3722	0.4031	0.4057	0.4053
1.95	0.2613	0.2731	0.3030	0.2998	0.2994
2.10	0.1854	0.1932	0.2215	0.2135	0.2078
2.25	0.1241	0.1296	0.1565	0.1452	0.1396
2.40	0.0785	0.0816	0.1060	0.0924	0.0875
2.55	0.0449	0.0461	0.0676	0.0531	0.0530
2.70	0.0190	0.0198	0.0390	0.0248	0.0249
2.85	0.0040	0.0035	0.0185	0.0056	0.0057
3.00	-0.0071	-0.0074	0.0047	-0.0066	-0.0065
3.15	-0.0124	-0.0128	-0.0040	-0.0135	-0.0134
3.30	-0.0149	-0.0157	-0.0089	-0.0166	-0.0166
3.45	-0.0166	-0.0164	-0.0111	-0.0172	-0.0171
3.60	-0.0148	-0.0152	-0.0114	-0.0160	-0.0160
3.75	-0.0125	-0.0127	-0.0106	-0.0140	-0.0140
3.90	-0.0105	-0.0104	-0.0092	-0.0115	-0.0115
4.05	-0.0073	-0.0079	-0.0075	-0.0090	-0.0090
4.20	-0.0061	-0.0058	-0.0059	-0.0067	-0.0067
4.35	-0.0036	-0.0039	-0.0043	-0.0047	-0.0047
4.50	-0.0026	-0.0026	-0.0030	-0.0031	-0.0031
4.65	-0.0026	-0.0021	-0.0020	-0.0018	-0.0018
4.80	-0.0005	-0.0009	-0.0012	-0.0009	-0.0009
4.95	-0.0007	-0.0002	-0.0006	-0.0003	-0.0003
5.10	-0.0004	-0.0004	-0.0002	0.0001	0.0001
5.25	0.0004	0.0002	0.0001	0.0004	0.0003
5.40	0.0000	0.0006	0.0003	0.0005	0.0005
5.55	0.0006	0.0003	0.0003	0.0005	0.0005
5.70	0.0000	0.0004	0.0004	0.0004	0.0004
5.85	0.0006	0.0009	0.0004	0.0000	0.0000
6.00	0.0017	0.0014	0.0003	0.0000	0.0000

Table 3.  $B^a(s)$  of LiH,  $\langle 100 \rangle$ -direction, experiment vs. theory. Experimental error:  $1.3 \cdot 10^{-3} (s > 2 \text{ \AA}) \leq \sigma \leq 9.5 \cdot 10^{-3} (s = 0.75 \text{ \AA})$ .

$s/\text{\AA}$	$B^a(s)$					
	(exp.)	SOSTIO	SOGTIO	MCS	EBS	EBS+d
0.00	3.9976	3.9673	3.9999	4.0000	4.0000	4.0000
0.15	3.6970	3.7683	3.7932	3.7946	3.7973	3.7973
0.30	3.1905	3.3120	3.3251	3.3217	3.3375	3.3375
0.45	2.6689	2.7998	2.7970	2.7846	2.8173	2.8174
0.60	2.2055	2.3281	2.3113	2.2926	2.3373	2.3374
0.75	1.8119	1.9254	1.8991	1.8792	1.9270	1.9271
0.90	1.4832	1.5899	1.5585	1.5399	1.5847	1.5847
1.05	1.2170	1.3085	1.2766	1.2592	1.2981	1.2980
1.20	0.9874	1.0695	1.0403	1.0238	1.0546	1.0543
1.35	0.7934	0.8650	0.8398	0.8240	0.8446	0.8442
1.50	0.6230	0.6888	0.6684	0.6534	0.6624	0.6618
1.65	0.4733	0.5383	0.5222	0.5079	0.5049	0.5042
1.80	0.3530	0.4113	0.3988	0.3856	0.3708	0.3700
1.95	0.2528	0.3066	0.2973	0.2852	0.2601	0.2592
2.10	0.1673	0.2222	0.2170	0.2058	0.1725	0.1715
2.25	0.1067	0.1562	0.1558	0.1452	0.1064	0.1055
2.40	0.0618	0.1060	0.1096	0.1000	0.0587	0.0577
2.55	0.0301	0.0691	0.0751	0.0669	0.0256	0.0247
2.70	0.0079	0.0427	0.0495	0.0431	0.0042	0.0033
2.85	-0.0048	0.0247	0.0309	0.0264	-0.0085	-0.0093
3.00	-0.0116	0.0128	0.0177	0.0151	-0.0149	-0.0155
3.15	-0.0134	0.0054	0.0089	0.0078	-0.0169	-0.0173
3.30	-0.0144	0.0013	0.0033	0.0032	-0.0160	-0.0164
3.45	-0.0123	-0.0008	0.0002	0.0007	-0.0135	-0.0138
3.60	-0.0089	-0.0015	-0.0012	-0.0005	-0.0102	-0.0105
3.75	-0.0065	-0.0015	-0.0015	-0.0010	-0.0068	-0.0070
3.90	-0.0045	-0.0011	-0.0012	-0.0009	-0.0037	-0.0038
4.05	-0.0017	-0.0005	-0.0006	-0.0007	-0.0011	-0.0011
4.20	0.0006	0.0000	-0.0002	-0.0004	0.0009	0.0010
4.35	0.0027	0.0004	0.0001	-0.0001	0.0023	0.0024
4.50	0.0028	0.0007	0.0004	0.0001	0.0031	0.0032
4.65	0.0039	0.0008	0.0006	0.0002	0.0034	0.0036
4.80	0.0038	0.0009	0.0008	0.0003	0.0034	0.0036
4.95	0.0036	0.0008	0.0009	0.0003	0.0032	0.0033
5.10	0.0030	0.0007	0.0009	0.0003	0.0028	0.0029
5.25	0.0025	0.0006	0.0009	0.0003	0.0023	0.0024
5.40	0.0020	0.0005	0.0008	0.0002	0.0018	0.0020
5.55	0.0013	0.0004	0.0008	0.0002	0.0014	0.0015
5.70	0.0008	0.0003	0.0007	0.0001	0.0011	0.0011
5.85	0.0012	0.0002	0.0006	0.0001	0.0008	0.0008
6.00	-0.0004	0.0001	0.0005	0.0001	0.0000	0.0006

- Aikala uses a free-ion wave function for  $\text{Li}^+$  published by Clementi [18] plus a variational  $1s$ -STO for  $\text{H}^-$  (Paakkari et al. [22] report a value of  $\alpha=0.6875$  for this function) for his SOSTIOs;
- MCS (minimal closed shell) is a 4GTO best-fit approximation to  $1s$ -STOs with  $\alpha(\text{Li}^+) = 2.6875$  and  $\alpha(\text{H}^-) = 0.77242$ , respectively (published in [8]) – the latter wave-function exponent was obtained by Hurst [23] for a hydride ion in a lattice of point charges;
- EBS (extended basis set) possesses p-type polarisation functions on both ions [8].

In the  $\langle 100 \rangle$ -direction, the first-order calculation is particularly insufficient to take into account the solid-state effect (including covalency at the nearest cation–anion distance), whereas the infinite-order Hartree-Fock calculation yields a  $B(s)$  close to the experiment (Figs. 2 and 6) provided polarisation functions are included (EBS). In the  $\langle 110 \rangle$ -direction, the Hartree-Fock results offer only a small improvement with respect to first-order calculations, still leaving a significant discrepancy with the experiment (Figs. 3 and 7). In the  $\langle 111 \rangle$ -direction with the largest interionic distance the agreement is much better for both types of



Table 4.  $B^a(s)$  of LiH,  $\langle 110 \rangle$ -direction, experiment vs. theory. Experimental error:  $1.3 \cdot 10^{-3} (s > 2 \text{ \AA}) \leq \sigma \leq 9.5 \cdot 10^{-3} (s = 0.75 \text{ \AA})$ .

$s/\text{\AA}$	$B^a(s)$					
	(exp.)	SOSTIO	SOGTIO	MCS	EBS	EBS + d
0.00	3.9974	3.9685	3.9999	4.0002	4.0000	4.0000
0.15	3.6930	3.7692	3.7932	3.7947	3.7973	3.7973
0.30	3.1869	3.3120	3.3251	3.3218	3.3375	3.3376
0.45	2.6662	2.7989	2.7973	2.7849	2.8175	2.8176
0.60	2.2013	2.3270	2.3122	2.2934	2.3381	2.3382
0.75	1.8078	1.9251	1.9013	1.8811	1.9288	1.9289
0.90	1.4808	1.5919	1.5628	1.5434	1.5884	1.5884
1.05	1.2176	1.3143	1.2840	1.2652	1.3051	1.3051
1.20	0.9911	1.0800	1.0517	1.0331	1.0664	1.0662
1.35	0.8021	0.8803	0.8560	0.8371	0.8629	0.8626
1.50	0.6373	0.7082	0.6897	0.6703	0.6886	0.6882
1.65	0.4937	0.5600	0.5478	0.5280	0.5396	0.5392
1.80	0.3807	0.4332	0.4268	0.4071	0.4133	0.4129
1.95	0.2834	0.3262	0.3241	0.3053	0.3077	0.3063
2.10	0.1978	0.2371	0.2378	0.2210	0.2209	0.2206
2.25	0.1359	0.1644	0.1665	0.1526	0.1511	0.1509
2.40	0.0867	0.1065	0.1089	0.0985	0.0966	0.0965
2.55	0.0494	0.0617	0.0638	0.0570	0.0553	0.0552
2.70	0.0226	0.0280	0.0297	0.0264	0.0252	0.0252
2.85	0.0047	0.0039	0.0051	0.0046	0.0041	0.0041
3.00	-0.0081	-0.0124	-0.0120	-0.0101	-0.0100	-0.0100
3.15	-0.0140	-0.0225	-0.0229	-0.0193	-0.0186	-0.0187
3.30	-0.0175	-0.0276	-0.0285	-0.0239	-0.0230	-0.0232
3.45	-0.0197	-0.0292	-0.0302	-0.0252	-0.0244	-0.0246
3.60	-0.0193	-0.0284	-0.0293	-0.0242	-0.0237	-0.0239
3.75	-0.0177	-0.0259	-0.0267	-0.0218	-0.0217	-0.0219
3.90	-0.0151	-0.0226	-0.0233	-0.0188	-0.0189	-0.0192
4.05	-0.0142	-0.0189	-0.0196	-0.0156	-0.0159	-0.0162
4.20	-0.0110	-0.0153	-0.0160	-0.0125	-0.0130	-0.0132
4.35	-0.0083	-0.0120	-0.0128	-0.0097	-0.0102	-0.0104
4.50	-0.0055	-0.0091	-0.0099	-0.0072	-0.0078	-0.0079
4.65	-0.0029	-0.0067	-0.0074	-0.0052	-0.0058	-0.0059
4.80	-0.0023	-0.0047	-0.0055	-0.0036	-0.0041	-0.0042
4.95	-0.0006	-0.0032	-0.0039	-0.0024	-0.0028	-0.0029
5.10	-0.0005	-0.0021	-0.0027	-0.0014	-0.0019	-0.0019
5.25	-0.0013	-0.0013	-0.0017	-0.0008	-0.0012	-0.0011
5.40	-0.0012	-0.0007	-0.0011	-0.0003	-0.0007	-0.0006
5.55	-0.0002	-0.0003	-0.0006	0.0000	-0.0003	-0.0003
5.70	-0.0005	-0.0001	-0.0003	0.0002	-0.0001	-0.0001
5.85	0.0008	0.0001	-0.0001	0.0003	0.0000	0.0001
6.00	0.0001	0.0002	0.0001	0.0003	0.0001	0.0001

Table 5.  $B^a(s)$  of LiH,  $\langle 111 \rangle$ -direction, experiment vs. theory. Experimental error:  $9.6 \cdot 10^{-4} (s > 2 \text{ \AA}) \leq \sigma \leq 1.00 \cdot 10^{-2} (s = 0.75 \text{ \AA})$ .

$s/\text{\AA}$	$B^a(s)$					
	(exp.)	SOSTIO	SOGTIO	MCS	EBS	EBS + d
0.00	3.9977	3.9693	3.9999	4.0002	4.0000	4.0000
0.15	3.6917	3.7699	3.7932	3.7947	3.7973	3.7973
0.30	3.1808	3.3125	3.3252	3.3219	3.3375	3.3376
0.45	2.6588	2.7992	2.7974	2.7850	2.8176	2.8177
0.60	2.1939	2.3271	2.3125	2.2937	2.3383	2.3384
0.75	1.8012	1.9253	1.9019	1.8816	1.9293	1.9294
0.90	1.4751	1.5926	1.5640	1.5444	1.5894	1.5895
1.05	1.2130	1.3158	1.2861	1.2670	1.3069	1.3069
1.20	0.9890	1.0827	1.0549	1.0358	1.0691	1.0691
1.35	0.8022	0.8845	0.8606	0.8410	0.8668	0.8668
1.50	0.6401	0.7139	0.6960	0.6757	0.6938	0.6940
1.65	0.4989	0.5674	0.5562	0.5352	0.5464	0.5466
1.80	0.3875	0.4424	0.4377	0.4163	0.4217	0.4221
1.95	0.2925	0.3372	0.3378	0.3169	0.3176	0.3183
2.10	0.2090	0.2500	0.2547	0.2352	0.2324	0.2333
2.25	0.1479	0.1794	0.1867	0.1693	0.1640	0.1651
2.40	0.0996	0.1237	0.1321	0.1174	0.1105	0.1118
2.55	0.0628	0.0810	0.0896	0.0779	0.0700	0.0714
2.70	0.0359	0.0494	0.0574	0.0486	0.0404	0.0418
2.85	0.0182	0.0268	0.0339	0.0279	0.0197	0.0211
3.00	0.0059	0.0116	0.0177	0.0138	0.0060	0.0074
3.15	-0.0021	0.0019	0.0070	0.0049	-0.0023	-0.0011
3.30	-0.0072	-0.0036	0.0005	-0.0003	-0.0067	-0.0056
3.45	-0.0086	-0.0064	-0.0033	-0.0030	-0.0085	-0.0075
3.60	-0.0087	-0.0073	-0.0054	-0.0042	-0.0086	-0.0077
3.75	-0.0071	-0.0070	-0.0064	-0.0045	-0.0077	-0.0069
3.90	-0.0056	-0.0062	-0.0067	-0.0042	-0.0063	-0.0057
4.05	-0.0046	-0.0052	-0.0063	-0.0036	-0.0048	-0.0042
4.20	-0.0039	-0.0040	-0.0054	-0.0028	-0.0034	-0.0029
4.35	-0.0025	-0.0029	-0.0044	-0.0019	-0.0022	-0.0017
4.50	-0.0015	-0.0020	-0.0033	-0.0012	-0.0012	-0.0008
4.65	-0.0005	-0.0012	-0.0022	-0.0005	-0.0004	-0.0001
4.80	0.0000	-0.0005	-0.0013	0.0000	0.0001	0.0004
4.95	0.0019	0.0000	-0.0006	0.0004	0.0004	0.0007
5.10	0.0016	0.0003	-0.0001	0.0006	0.0006	0.0009
5.25	0.0009	0.0005	0.0003	0.0007	0.0007	0.0009
5.40	0.0013	0.0006	0.0005	0.0008	0.0007	0.0009
5.55	0.0007	0.0006	0.0006	0.0008	0.0006	0.0008
5.70	0.0014	0.0005	0.0006	0.0007	0.0005	0.0007
5.85	0.0017	0.0004	0.0006	0.0006	0.0004	0.0006
6.00	0.0014	0.0003	0.0006	0.0005	0.0003	0.0005

calculation (Figs. 4 and 8). The spherically averaged curves are shown in Figure 5.

Furthermore, the Slater vs. Gaussian effect is visible, but does not affect the overall discussion of the results for the  $\langle 100 \rangle$  and the  $\langle 110 \rangle$ -direction.

It is possible to assume that addition of a d-shell centred on the  $\text{H}^-$  sites to the EBS ( $\alpha = 0.3$ ) would take into account polarisation owing to the second coordination sphere (which consists of twelve ions with an electrical charge of the same sign as the central reference ion), thus improving the agreement with experiment in the  $\langle 110 \rangle$ -direction without having much in-

fluence on  $B(s)$  in the other directions. In order to test this hypothesis the directional  $B(s)$  corresponding to this basis set were calculated and also compared to the EBS results (Figures 6–8). Obviously, the suggested effect upon the overall symmetry of the crystal wave function is negligible. A variation of the d-shell exponent in the range  $0.15 \leq \alpha \leq 0.4$  resulted in no further change in  $B(s)$ . With the EBS we are apparently already very close to the Hartree-Fock limit; the remaining discrepancies have thus to be associated with fundamental shortcomings of the one-electron picture, i.e. with correlation effects. Owing to the low electron

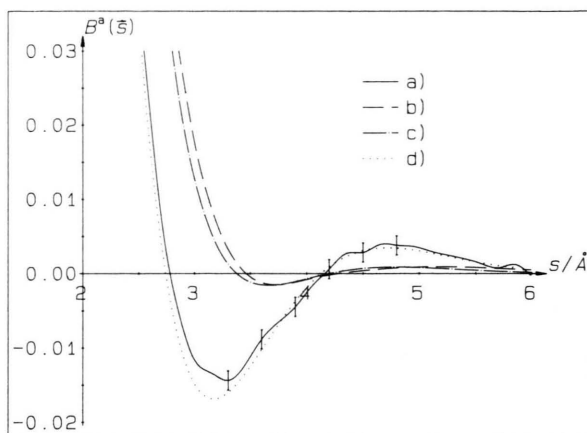


Fig. 2.  $B^a(s)$  of LiH,  $\langle 100 \rangle$ -direction, theory vs. experiment: a) experiment; b) SOGTIOs; c) SOSTIOs of Aikala [6]; d) CRYSTAL with EBS.

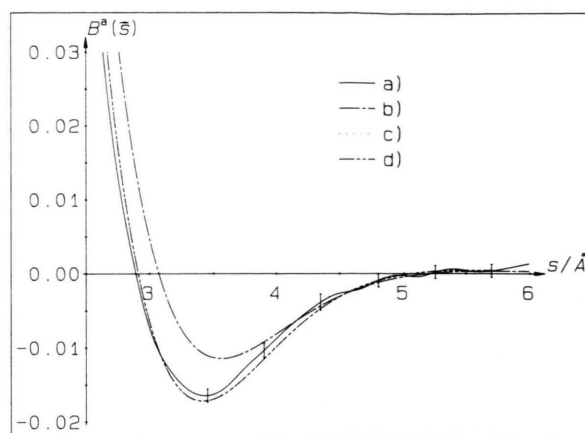


Fig. 5.  $B^a(s)$  of LiH, spherical average, theory vs. experiment: a) experiment, b) CRYSTAL with MCS; c) CRYSTAL with EBS, d) CRYSTAL with EBS + d-shell polarisation functions at  $H^-$  sites.

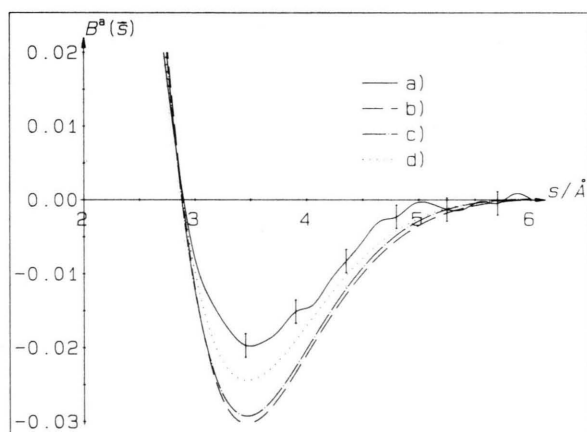


Fig. 3.  $B^a(s)$  of LiH,  $\langle 110 \rangle$ -direction, theory vs. experiment. Line styles a)–d) as in Figure 2.

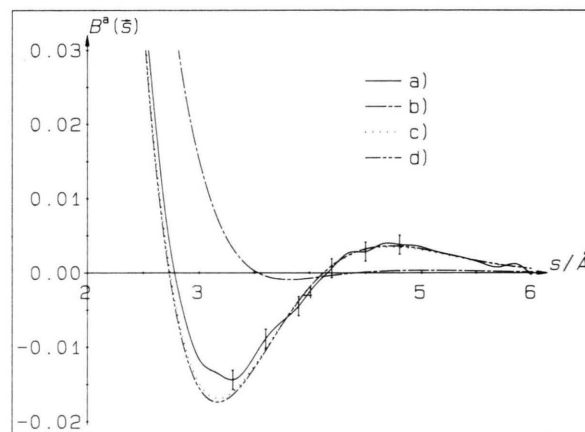


Fig. 6.  $B^a(s)$  of LiH,  $\langle 100 \rangle$ -direction, theory vs. experiment. Line styles a)–d) as in Fig. 5.

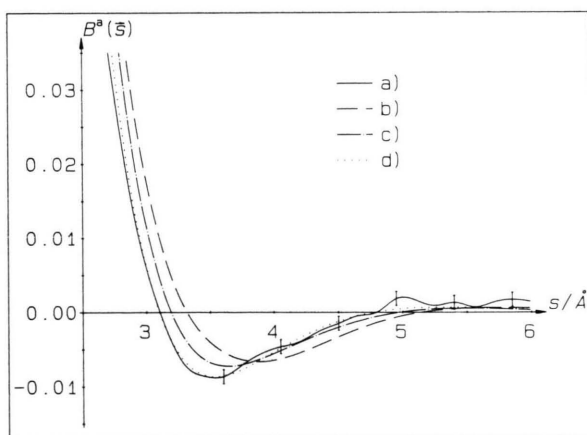


Fig. 4.  $B^a(s)$  of LiH,  $\langle 111 \rangle$ -direction, theory vs. experiment. Line styles a)–d) as in Figure 2.

density in crystalline LiH, they can be expected to be rather significant.

## 5. Conclusion

In the present work we have tried to show that in the case of LiH it is now possible to differentiate quantitatively between various theoretical solid-state models with respect to Compton profile measurements, especially when the Compton profiles are transformed into the position-space representation. Our investigation confirms by and large the ionic picture of the bonding in LiH (in agreement with the X-ray diffraction mea-

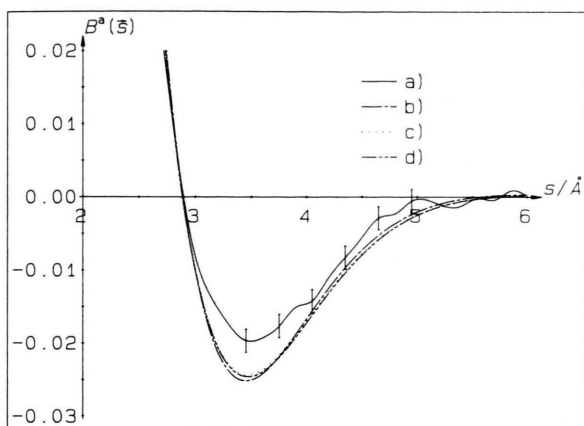


Fig. 7.  $B^a(s)$  of LiH,  $\langle 110 \rangle$ -direction, theory vs. experiment. Line styles as in Figure 6.

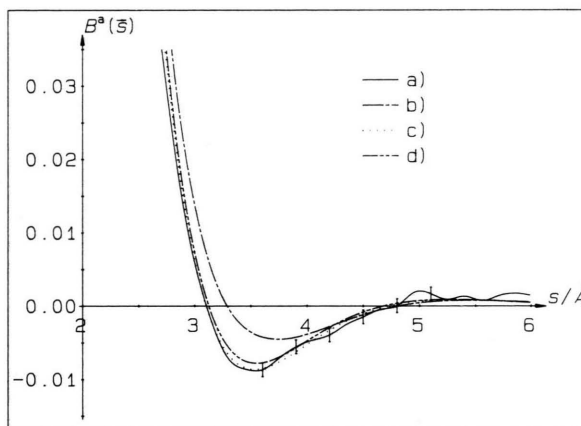


Fig. 8.  $B^a(s)$  of LiH,  $\langle 111 \rangle$ -direction, theory vs. experiment. Line styles as in Figure 6.

surements of Calder et al. [24], corroborated by Vidal and Vidal-Valat [25, 26]). Nevertheless, covalency (incomplete charge transfer from lithium to hydrogen in the atomic or backbonding from  $H^-$  to  $Li^+$  in the ionic picture) and polarisation of the crystal wave function have to be considered as well. However, owing to the presence of numerous neighbouring atoms, which already provide basis functions for symmetry-adapted polarisation, it is not necessary to include a large number of angular polarisation functions. Finally, the remaining discrepancies between the experiment

and the Hartree-Fock calculation with a sufficiently saturated basis set point out the importance of electron-electron correlation also in an ionic crystal such as LiH.

#### Acknowledgements

We gratefully acknowledge the continuous financial support by the Fonds der Chemischen Industrie. One of us (T.A.) is indebted to the Stifterverband der Wissenschaft for a Graduation Award.

- [1] P. Pattison, W. Weyrich, and B. G. Williams, *Solid State Commun.* **21**, 1967 (1977).
- [2] W. Weyrich, *Habilitationsschrift*, Darmstadt 1978.
- [3] P. Pattison and W. Weyrich, *J. Phys. Chem. Solids* **40**, 213 (1979).
- [4] K.-F. Berggren, Report No. LiH-IFM-IS-40, Department of Physics, Linköping University, Linköping, Sweden 1975.
- [5] G. Grosso, G. Pastori Parravicini, and R. Resta, *phys. stat. sol. (b)* **73**, 371 (1976).
- [6] O. Aikala, *J. Phys. C: Solid State Phys.* **9**, L131 (1976).
- [7] W. A. Reed, *Phys. Rev. B* **18**, 1986 (1978).
- [8] R. Dovesi, C. Ermondi, E. Ferrero, C. Pisani, and C. Roetti, *Phys. Rev. B* **29**, 3591 (1984).
- [9] V. N. Kotova, G. G. Larikova, N. I. Zamyatnina, and L. P. Dykina, *Zh. Anal. Khim.* **34**, 1651 (1979), English edition **34**, 1280 (1980).
- [10] E. Heuser, *Dissertation*, Darmstadt 1982, p. 187.
- [11] W. Weyrich, *Ber. Bunsenges. Phys. Chem.* **79**, 1085 (1975).
- [12] P. Bachmann, *Diplomarbeit*, Darmstadt 1976, p. 51 ff.
- [13] C. Pisani, R. Dovesi, and C. Roetti, *Hartree-Fock ab initio Treatment of Crystalline Systems*, Springer-Verlag, Berlin 1988, p. 15 ff.
- [14] M. Bräuchler, S. Lunell, I. Olovsson, and W. Weyrich, *Int. J. Quantum Chem.* **35**, 895 (1989).
- [15] P.-O. Löwdin, *A Theoretical Investigation into Some Properties of Ionic Crystals*, Almqvist & Wiksells Boktryckeri, Uppsala 1948.
- [16] P.-O. Löwdin, *Adv. Phys.* **5**, 1 (1956).
- [17] K. Sasagane, K. Mori, A. Ichihara, and R. Itoh, *J. Chem. Phys.* **92**, 3619 (1990).
- [18] E. Clementi, *Tables of Atomic Functions*, Suppl. IBM J. Res. Dev. **9**, 2 (1965).
- [19] C. C. Roothaan and G. A. Soukup, *Int. J. Quantum Chem.* **15**, 449 (1979).
- [20] S. F. Boys and F. Bernardi, *Mol. Phys.* **19**, 553 (1970).
- [21] G. Alagona, C. Ghio, R. Cammi, and J. Tomasi, *Int. J. Quantum Chem.* **32**, 207 (1987).
- [22] T. Paakkari, V. Halonen, and O. Aikala, *Phys. Rev. B* **13**, 4602 (1976).
- [23] R. P. Hurst, *Phys. Rev.* **114**, 746 (1959).
- [24] R. S. Calder, W. Cochran, D. Griffiths, and R. D. Lowde, *J. Phys. Chem. Solids* **23**, 621 (1962).
- [25] J.-P. Vidal and G. Vidal-Valat, *Acta Cryst. B* **42**, 131 (1986).
- [26] G. Vidal-Valat, J.-P. Vidal, K. Kurki-Suonio, and R. Kurki-Suonio, *Acta Cryst. A* **48**, 46 (1992).